

A New Technique for Proppant Schedule Design

E.V. Dontsov and A.P. Peirce, Department of Mathematics, University of British Columbia

Abstract

This study introduces a novel methodology for the design of the proppant pumping schedule for a hydraulic fracture, in which the final proppant distribution along the crack is prescribed. While the design is based on the assumption that the particles have relatively weak impact on the fracture propagation, the validity of this assumption can be tested *a posteriori*. This makes it possible to relate the proppant velocity to the clear fluid velocity inside the fracture, which is calculated assuming no proppant. Having the history of the clear fluid velocity distribution, the prospective proppant motion can be computed. Volume balance is then used to relate the final concentration at some point inside the fracture to the corresponding input concentration at a specific time instant, which helps to avoid solving an inverse problem. One exceptional feature of the approach lies in the fact that it is applicable to multiple fracture geometries and can be implemented using various hydraulic fracturing simulators. To verify the technique, two fracture geometries are considered - Khristianovich-Zhel'tov-Geertsma-De Klerk (KGD) and pseudo-3D (P3D). It is shown that the developed approach is capable of properly estimating the pumping schedule for both geometries. In particular, the proppant placement along the fracture at the end of the pumping period, calculated according to the adopted proppant transport model, shows close agreement with the design distribution. Comparison with Nolte's scheduling scheme shows that the latter is not always accurate, and cannot capture the essential differences between the schedules for the fracture geometries considered.

Introduction

Hydraulic fracturing (HF) is a process in which a viscous fluid that is injected into a fracture drives crack propagation. Use of proppant prevents complete closure of the fracture after pumping has stopped and the fluid has leaked off. Despite the fact that many studies have been devoted to proppant transport modelling and investigating the effects of settling, Daneshy (1978), Mobbs and Hammond (2001), Shokir and Al-Quraishi (2007), only a few consider the design of a proppant schedule Crawford (1983), Nolte (1986), Meng and Brown (1987), Gu and Desroches (2003). The appropriate proppant schedule is as important as the correct prediction of the fracture footprint, since it directly affects the proppant distribution inside the fracture, and thus influences the conductivity and the production rate.

One of the most common approaches for generating the pumping schedule is a protocol developed by Nolte (1986). This is a very convenient method, as it provides an analytical formula for the schedule for a given efficiency, total pumping time, and a desired (uniform) concentration inside the fracture at the end of the job. The approach is based on the conservation of volume, and the estimation of the total volume of fluid that leaks off during the HF treatment. A power-law type schedule is then suggested and the exponent is calculated based on the proppant volume balance. Not being tied to any fracture geometry, this scheduling approach is considered applicable to multiple fracture geometries, such as PKN or radial. The universality, the consistency with the global balance laws, and the ease of use are possibly the main reasons why this scheduling methodology is commonly used, see e.g. Economides and Nolte (2000), Rahman and Rahman (2010). There is an alternative method, developed in Gu and Desroches (2003), which suggests using an iterative scheme together with an appropriate proppant transport model to solve an inverse problem to generate a pumping schedule. The basis of that procedure is to divide the schedule into intervals and then adjust the input concentration values iteratively based on the results of the forward problem solution using the previous schedule. In principle,

this iterative algorithm can yield the most accurate solution, however the accuracy and the required computational resources depend heavily on the complexity of the forward model.

It would be desirable to develop a proppant scheduling methodology that is more accurate than Nolte's method, but less computationally challenging than the iterative procedure described by Gu and Desroches. To facilitate this, the proppant is assumed to have a minor impact on fracture propagation. This allows us to avoid an iterative scheme and lengthy simulations with proppant transport. At the same time, the influence of the fracture geometry and other features that can be built into a HF simulator are taken into account. One of the biggest advantages of the proposed technique is its applicability to various HF simulators, which do not need the ability to model the proppant transport itself, see the examples of such simulators in Adachi et al. (2007), Peirce and Detournay (2008).

The paper is organized as follows: Section 2 outlines the procedure for the method; then Sections 3 and 4 illustrate the implementation for KGD and P3D fracture geometries, respectively; and, finally, Section 5 compares different schedules (including Nolte's schedule) and discusses the applicability and possible extensions of the approach.

Idea behind estimation of pumping schedule

Assume that the properties of the rock, the fluid and the proppant, as well as the pumping rate are all known and fixed. Before a pumping schedule can be designed, the following target characteristics need to be prescribed by the user:

- i. the geometry of the hydraulic fracture (HF), which can be interpreted as the type of HF model that is used for the design, such as KGD, radial, PKN, P3D, or a fully planar HF solver.

- ii. the size of the fracture at the end of pumping, which is nominally the half-length (or radius) of the HF.
- iii. the desired proppant distribution inside the fracture at the end of the job.

Since it is unclear what the optimal proppant pattern should be, item (iii) could, in itself could be a separate topic for research; see e.g. Neto and Kotousov (2013) where the residual fracture opening supported by proppant is analyzed, or Cipolla et al. (2009) where the effect of the proppant distribution on the conductivity is studied. Thus, investigating the optimal proppant pattern is beyond the scope of this study. It is therefore assumed that the desired distribution of the proppant concentration is prescribed or known. Thus the schedule design process should be sufficiently adaptable to be able to accommodate any desired proppant distribution.

The main objective of this study is the calculation of the pumping schedule for given material properties, HF geometry, the design length of the HF, and the desired proppant distribution at the end of the fracturing job.

To design the pumping schedule, it is imperative to know where the proppant would be transported to. This can be achieved by estimating the proppant velocity inside the fracture as a function of time and space. At the same time, assuming that the proppant concentrations are sufficiently small (i.e. that the particles have small impact on the fracture propagation), the proppant velocity can be related to the fluid velocity, where the latter is calculated assuming *no proppant*. Consequently, the tentative procedure for the pumping schedule design is:

- i. run an appropriate HF solver *without proppant*, record time histories of all velocity components, width and fracture footprint, and find the time required to achieve the desired fracture size/ footprint,
- ii. find the location of the proppant injected at time instant t_i by “tracking” its position with time by integrating the actual velocity field, and
- iii. use conservation of volume to relate the input concentration (at any given time t_i) to the concentration at the end of pumping.

It is important to note, that this procedure is applicable to *any* HF solver and can be implemented as a separate module. Also, the solution for the proppant location resembles the Lagrangian approach used in continuum mechanics, and has a clear advantage over the “classical” Eulerian approach (i.e. solving the advection equation for proppant transport), by making it possible to relate the final proppant distribution to the schedule concentration. Another important advantage of the proposed approach is that *any* desired concentration distribution can be achieved through the appropriate scheduling, which opens interesting research possibilities for the optimal proppant placement inside the HF.

To illustrate the methodology, two fracture geometries are examined: KGD and P3D. The schedules for both are verified numerically by using a proppant transport model described in Dontsov and Peirce (2014).

Pumping schedule for KGD fractures

To address the proppant scheduling problem in a more straightforward way, the one-dimensional KGD fracture geometry is analyzed first. Given the properties of the rock and the fracture design

half-length l_e , an appropriate HF simulator (without the proppant) can be used to deduce the total injection time t_e , as well as to record the histories of the fracture footprint $l(t)$, width $w(x,t)$, and average fluid velocity $V_f(x,t)$, where x is the coordinate along the fracture. Due to the nonuniform distribution of the proppant across the fracture width, the average proppant velocity is higher than that of the slurry. It follows from Dontsov and Peirce (2014) in the limit of low concentrations, that the ratio between these two corresponding velocities is $\beta = 1.2$. This can be understood in the following way: the proppant tends to concentrate near the center of a channel, where it flows with nearly the maximum velocity, which is always higher than the average velocity in the channel. By denoting the position of the particles at time t , injected at t_i , by $x(t,t_i)$, the governing equation for the proppant front is

$$\frac{\partial x}{\partial t} = \beta V_f(x,t), \quad x(t_i, t_i) = 0, \quad t_i \leq t \leq t_e, \quad (1)$$

where the parameter β enters the problem through the initial condition, so that (1) is actually an ordinary differential equation. It is also implicitly stated that the coordinate x originates from the wellbore and that the proppant enters the fracture (not the wellbore) at time t_i . The solution of (1) allows us to find $x(t,t_i)$, i.e., the current location of the proppant, which is injected at any time t_i .

Fig. 1 shows schematics of proppant front movement in the fracture. Here ϕ is the proppant volume fraction, Q_0 is the slurry injection rate, while x is the coordinate along the fracture. The schedule for the proppant injection concentration is shown in the top right picture, and the red area is proportional to the total amount of proppant pumped during the interval Δt , which is equal to $\phi_0 Q_0 \Delta t$. This proppant (injected over time Δt) is schematically shown at $t=t_i$ in the top left picture. At this time instant the particles leave the borehole and enter the fracture. At time $t > t_i$, the same proppant (half of it due to symmetry) is inside the fracture, as shown in the bottom picture. To calculate the “pad” time, t_p , (the time up to which pure fluid is pumped and before the proppant injection) one may use the solution for $x(t,t_i)$ and require

$$x(t_e, t_p) = l_e, \quad (2)$$

i.e. determine t_p by requiring that the particles reach the crack tip by the end of pumping. Note that for a more accurate prediction for larger diameter proppant, it is reasonable to replace l_e in (2) by a smaller length, \bar{l}_e , where the latter is calculated based on

$$w(\bar{l}_e, t_e) = 6a, \quad (3)$$

where a is the particle radius. This ensures that the proppant bridging criterion (i.e. a minimum fracture width of 3 particle diameters) is satisfied and that there is no proppant in the tip region. Given the prescribed proppant concentration distribution inside the fracture, $\phi_d(x)$, the balance of mass can be used to obtain

$$\frac{1}{2} Q_0 \phi(t_i) \Delta t = w(x(t_e, t_i), t_e) [x(t_e, t_i) - x(t_e, t_i + \Delta t)] \phi_d(x(t_e, t_i)), \quad (4)$$

where the left side reflects the volume of the proppant injected between t_i and $t_i + \Delta t$ (the 1/2 factor comes from the symmetry), while the right side calculates the same volume at the end of the fracturing job. By taking a limit of $\Delta t \rightarrow 0$ in (4), the result can be simplified to

$$\phi(t_i) = -\frac{2w(x(t_e, t_i), t_e)}{Q_0} \frac{\partial x(t_e, t_i)}{\partial t_i} \phi_d(x(t_e, t_i)), \quad t_i > t_p, \quad (5)$$

which allows us to calculate the proppant schedule for any desired concentration distribution along the fracture. Note that due to the 1D nature of the geometry, Q_0 is the injection rate per unit length, i.e. measured in m^2/s . Also note that any function $\phi_d(x)$ can be used in (5), i.e. any proppant distribution can be achieved without introducing extra complexities. In addition, all specifics of the hydraulic fracturing model, such as leakoff or, possibly, stress barriers, are naturally accounted for by the fluid velocity field $V_f(x, t)$ and the fracture width $w(x, t)$, which then influence the solution of (1) and consequently the schedule through equation (5).

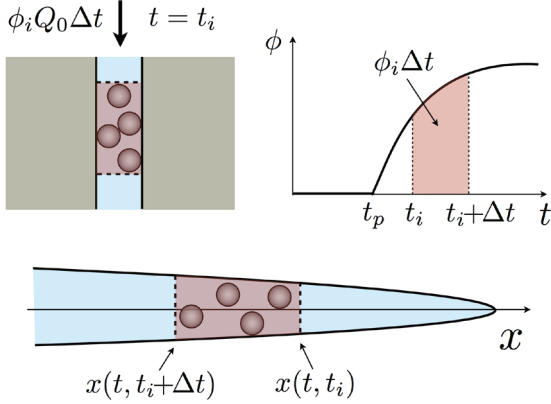


Figure 1. Schematics of the proppant schedule (top right), the proppant in the borehole at $t=t_i$ (top left) and the same proppant at time t in the KGD fracture (bottom picture).

Numerical examples. From the point of view of numerical implementation, the task of finding the pumping schedule according to (5) requires an appropriate numerical scheme for the solution of Eq.(1), numerical differentiation in Eq. (5), as well as an extensive use of interpolation. The interpolation is used in Eq. (1), since $V_f(x, t)$ is computed for a discrete set of x and t and in Eq. (5) for the evaluation of $w(x(t_e, t_i), t_e)$ and $\partial x(t_e, t_i) / \partial t_i$ (the x values are first interpolated and then differentiated numerically). To achieve high accuracy and to preclude possible oscillations (that can be caused by spline interpolation), the built-in Matlab function ‘‘PCHIP’’ (Piecewise Cubic Hermite Interpolating Polynomial) is used for the interpolation. To deal with the numerical solution of Eq. (1), a 4th order Runge-Kutta method is used.

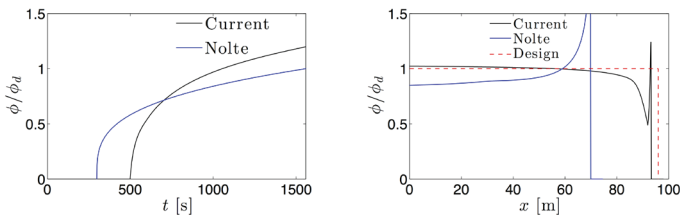


Figure 2. Left panel: pumping schedule calculated according to equation (5) and Nolte’s model with the efficiency $\eta=0.63$. Right panel: concentration distribution along a KGD fracture for the proposed and Nolte’s schedules.

To verify the proposed approach, an example problem is considered. As follows from Dontsov and Peirce (2014), the proppant transport model allows for simulation of fracture propagation by a slurry, which consists of a Newtonian fluid mixed with spherical particles. The selected

parameters for the example problem are $E'=25$ GPa for the plane strain modulus, $\mu=0.1$ Pa \cdot s for the shear viscosity of the fracturing fluid, $Q_0=10^{-3}$ m^2/s for the inlet flux, $C'=5 \times 10^{-5}$ $\text{m}/\text{s}^{1/2}$ for Carter’s total leakoff coefficient, $K_{IC}=1$ $\text{MPa} \cdot \text{m}^{1/2}$ for the fracture toughness and $a=0.2$ mm for the particle radius. The design length of the fracture is set to $l_c=100$ m, while the target concentration is considered to be uniform and is equal to $\phi_d = 0.2 \times \phi_m$. Here $\phi_m=0.585$ is the maximum volume concentration that can be achieved, Boyer et al. (2011), Dontsov and Peirce (2014). Note that, assuming the proppant mass density of 2300 kg/m^3 , this concentration can be translated to approximately 2.6 lb/gal. The HF simulator for KGD fractures, described in Dontsov and Peirce (2014), is used to calculate the duration of the HF treatment and to record the history of the average velocity without proppant, which is then used to calculate the schedule. Given the pumping schedule, the same simulator is used to verify the design.

Fig. 2 shows the schedule, calculated according to equation (5) and the concentration distribution along the fracture at the end of the simulation (black solid lines). In addition, these results are compared to Nolte’s scheduling from Nolte (1986) (blue solid lines). Note that Nolte’s model including the correction for the pad length is used; (see Appendix A for a description of Nolte’s pumping schedule). Despite using the correction, the prediction of Nolte’s model notably underestimates the pad size, which causes premature tip screen-out leading to a fracture length under 80 m (as opposed to the prescribed 100 m length). The current approach shows better performance, as it just slightly distorts the designed 100 m fracture length, and produces a nearly uniform concentration distribution along the fracture. Note that the propped length for the design concentration is under 100 m due to the condition enforced in (3). The spikes in the concentration correspond to plug formation, i.e. a zone where the proppant is compacted to nearly the maximum value that corresponds to the volume fraction of $\phi_m=0.585$. For the current schedule, the plug just started to form and therefore does not significantly affect the fracture propagation. The ‘‘dip’’ in the proppant distribution is due to both numerical diffusion and the effect of coupling between proppant transport and HF propagation, namely the change of the slurry viscosity with concentration. This ‘‘dip’’ is the result of assumption that particles produce small influence on the fracture propagation, and, at the same time, the discrepancy between the actual solution and the design highlights the error introduced by such an assumption. Note that the schedule for the proposed approach has a region in which the concentration exceeds ϕ_d , while the resultant concentration inside the fracture is approximately equal to ϕ_d . This is due to the fact that the ratio between particle and slurry velocities is $\beta=1.2$, which effectively reduces the mixture concentration by β when it reaches a steady flow (i.e., according to the proppant transport model assumptions, when it enters the fracture).

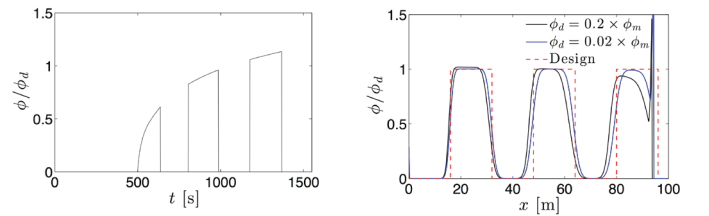


Figure 3. Pumping schedule and the corresponding concentration distribution along a KGD fracture for a ‘‘zebra’’ configuration.

To highlight the versatility of the proposed scheduling procedure, **Fig. 3** shows the pumping schedule and resultant proppant distribution for regular ($\phi_d = 0.2 \times \phi_m$) and small ($\phi_d = 0.02 \times \phi_m$) concentrations giving a ‘‘zebra’’ configuration. This configuration suggests that, at the end of

pumping, the proppant should be concentrated in three equal stripes, placed equidistantly inside the fracture. This increases the permeability, as hydrocarbons can flow between the bridges. In practice, this technique can use numerous pulses, while only three are considered here since a large number of pulses would require a much finer mesh, which is computationally demanding. As can be seen from the results, the calculated schedule indeed leads to the desired proppant placement with adequate accuracy. As was the case for Fig. 2, the discrepancy comes mainly from numerical diffusion and the coupling between HF propagation and proppant transport. Since the coupling is minimal for small concentrations, the blue line (which corresponds to the small concentration solution) can be used to estimate the discrepancy caused by the numerical scheme only. Hence, the difference between the solutions for regular and small concentrations indicates the effect of coupling. Even though the effect of coupling leads to visible differences, the overall accuracy of the approach is still satisfactory. It is important to note that higher concentrations can lead to bigger differences, which is the limitation of the proposed design approach. It is hard to estimate the universal upper bound for concentration, below which this approach gives accurate results since the accuracy may depend on the type of HF model and different levels of accuracy may be required in different cases. For this reason, it is imperative to verify the accuracy before treatment by performing a comparison similar to that in Fig. 2 or Fig. 3. At the same time, it is remarkable that the higher viscosity of the slurry (due to the presence of proppant) does not alter the final fracture length appreciably. This is because the biggest pressure gradients are near the fracture tip, where the width is very narrow, while the rest of the fracture is subject to smaller pressure gradients. When the proppant is introduced, the higher viscosity of the slurry perturbs mostly the small pressure gradients, which are away from the tip and thus does not significantly affect the pressure distribution and fracture propagation. When the proppant eventually reaches the tip region, it starts to disturb the fracture, but it is already too late since the fracturing job is over once the proppant reaches the crack tip. In other words, even though the particles change the viscosity of a slurry, the time interval during which the proppant can affect the fracture behavior is small, which makes the consequences of the coupling effect relatively insignificant. This statement is independent of fracture geometry and can also be extended to radial fractures, P3D fractures, or more general fracture geometries for example.

Pumping schedule for P3D fractures

The design of a pumping schedule for the P3D geometry (Adachi et al. (2010)) is conceptually similar to that for the KGD model, but there are several notable differences. One of them comes from the fact that a line source is used in the P3D model, as opposed to a point source. Another difference is related to the two-dimensional nature of the proppant flow, and the presence of a vertical velocity component. For the purpose of schedule calculation, it is assumed that the gravitational settling is negligible, and hence the vertical component of the velocity is zero along the x axis ($z=0$), see Fig. 4.

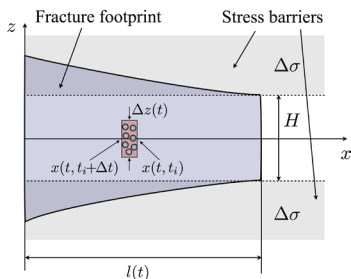


Figure 4. Schematics of the P3D fracture with the “proppant tracking box” indicated near the center of the fracture.

In this case, the proppant that is pumped in the vicinity of $z=0$ remains close to the x axis during the fracture growth. This fact allows us to “track” the proppant along the x axis and not to consider its vertical migration. The schematics of the P3D fracture together with the “proppant tracking box” are shown in the Fig. 4. This box is the area that is occupied by proppant, injected over time interval from t_i to $t_i + \Delta t_i$, which propagates together with particles as they move inside the fracture. The function $x(t, t_i)$ has the identical meaning as for the KGD fracture; it represents the position of the proppant at time t , that was injected at time t_i . As will be shown later, the height of the box, $\Delta z(t)$, varies with time due to the presence of the vertical velocity component. Since the particles can easily be traced along the x coordinate, it is natural to establish the target concentration along the x axis as well. As for the KGD fracture, the simulations without proppant are first performed, and for given problem parameters and design length, l_e , the pumping time t_e is calculated and the histories of the appropriate quantities are recorded. Knowing the history of the x component of the average fluid velocity at $z=0$, $V_{f,x}$, the motion of the particles can be described by solving

$$\frac{\partial x}{\partial t} = \beta V_{f,x}(x, t), \quad x(t_i, t_i) = 0, \quad t_i \leq t \leq t_e, \quad (6)$$

which is identical to (1). Also, the “pad” time, t_p , is calculated in a similar fashion as

$$x(t_e, t_p) = l_e,$$

where the final length of the fracture l_e can be replaced by \bar{l}_e for larger diameter proppant. Here \bar{l}_e is determined from

$$w(\bar{l}_e, t_e) = 6a,$$

where $w(x, t)$ is the fracture width along the x axis for $z=0$. With reference to Fig. 4, the volume of the proppant at the injection point and at the end of the fracture treatment can be equated to find

$$\begin{aligned} \phi(t_i) V_{f,x}(0, t_i) w(0, t_i) \Delta z(t_i) \Delta t = & [x(t_e, t_i) \\ & - x(t_e, t_i + \Delta t)] w(x(t_e, t_i), t_e) \Delta z(t_e) \phi_d(x(t_e, t_i)), \end{aligned} \quad (7)$$

where $\phi_d(x)$ is the design concentration distribution along the x -axis, is the average fluid velocity at the inlet (and $z=0$), while $w(0, t_i)$ is the corresponding width of the fracture at that point. By noting that

$$\frac{\Delta z(t_e)}{\Delta z(t_i)} = \beta \int_{t_i}^{t_e} \frac{\Delta V_{f,z}(x(t, t_i), t)}{\Delta z(t_i)} dt, \quad (8)$$

where $\Delta V_{f,z}$ is the difference between the vertical components of the fluid velocity at the top and bottom of the “proppant tracking box”, equation (7) can be simplified to

$$\begin{aligned} \phi(t_i) = & - \frac{w(x(t_e, t_i), t_e)}{w(0, t_i) V_{f,x}(0, t_i)} \frac{\partial x(t_e, t_i)}{\partial t_i} \left(1 \right. \\ & \left. + \beta \int_{t_i}^{t_e} \frac{\partial V_{f,z}(x(t, t_i), t)}{\partial z} dt \right) \phi_d(x(t_e, t_i)). \end{aligned} \quad (9)$$

Note that $\partial V_{f,z} / \partial z$ is evaluated at $z=0$ and its history has to be “pre-computed” in addition to the history of the horizontal velocity component, $V_{f,x}$. It is important to understand that β should not enter on the left side in (7), since the ratio between the proppant and slurry fluxes is $\phi(t_i)$, while the slurry flux is proportional to $V_{f,x}(0, t_i)$. At the

same time, since the proppant's vertical velocity (as opposed to the fluid's) is responsible for the vertical "box" growth, β appears in (8). As with the expression for the KGD fracture (5), the relation (9) can be used to design a proppant schedule for any target concentration profile along the x axis, $\phi_d(x)$. This adds versatility to the approach.

Numerical examples. To illustrate these developments for P3D fractures and to assess the validity of (9), several numerical examples are considered. The parameters used for the calculations are $E^*=25$ GPa for the plane strain modulus, $\mu=0.1$ Pa·s for the shear viscosity of the fracturing fluid, $Q_0 = 10^{-2}$ m³/s for the total inlet flux, $H = 25$ m for the reservoir layer, $\Delta\sigma = 2.5$ MPa for the magnitude of the stress barriers, $C^* = 5 \times 10^{-5}$ m/s^{1/2} for the Carter (total) leakoff coefficient, $K_{IC} = 1$ MPa·m^{1/2} for the fracture toughness, $a = 0.2$ mm for the particle radius, $g = 9.8$ m/s² for the gravitational acceleration and $\rho^p - \rho^f = 1300$ kg/m³ for the difference between particle and fluid mass densities. Refer to Fig.4 and Adachi et al. (2010), Dontsov and Peirce (2014) for more details. Note that the gravitational settling is formally included in the simulations, but, since a relatively small particle size is considered, there is almost no distortion in the symmetry due to settling. As noted in Dontsov and Peirce (2014), the dimensionless parameter that determines the settling extent is

$$G_s = \frac{16\Delta\sigma a^2 g Q_0 E'^3 (t_e - t_p)}{3\Delta\sigma^4 H^4},$$

where t_e is the total pumping time, while t_p is the time at which the proppant is first injected, as shown in the top right panel in Fig. 1. The parameter G_s reflects the ratio between proppant travel time and the settling time. When $G_s \gg 1$, then settling occurs before the end of pumping, while if $G_s \ll 1$, then, practically, gravity does not alter the particle distribution. For the set of parameters under consideration, $G_s = 0.035$, which indeed suppresses the effect of settling. As with the KGD fracture geometry, the design length of the fracture is set to $l_e = 100$ m, while the target concentration is considered to be uniform and is equal to $\phi_d = 0.2 \times \phi_m$, where $\phi_m = 0.585$. The HF simulator for P3D fractures, described in Dontsov and Peirce (2014), is used to calculate the duration of the HF treatment and to record the history of the average x component of the velocity and the derivative of the vertical velocity component (assuming no proppant), which are then used to calculate the schedule using (9). The same numerical techniques that were used for dealing with the KGD fracture scheduling in Section 3, are utilized for the numerical solution of (6) and for the interpolation, which are both necessary for the evaluation of (9). Given the pumping schedule, the same HF simulator for the P3D fracture, this time with proppant, is used to verify the efficacy of the design.

To evaluate the accuracy of the proposed scheduling, the top left panel in Fig. 5 compares the schedule that is calculated according to (9) with that suggested by Nolte (1986). The differences are similar to those found for the KGD model; namely, Nolte's approach underestimates both the time of the first proppant injection, t_p , and the maximum concentration near the end of pumping. The consequences are similar as well, i.e. Nolte's schedule leads to premature tip screen-out (which in turn leads to a shorter than desired fracture length) and smaller concentration near the inlet, see Fig. 5. With regard to the accuracy of the current approach, there is also a "dip" near the fracture tip and a small plug (i.e. zone where $\phi = \phi_m = 0.585$) starts to form thereafter. Despite the fact that P3D and KGD consider different types of fractures, the reasons for the "dip" are similar; namely, the coupling between proppant transport and HF propagation and numerical diffusion. Note that the term with the vertical velocity derivative in (9) plays an important role and its absence can lead to observable inaccuracy of the final concentration, while the t_p stays unaffected. Of course, the degree of influence depends

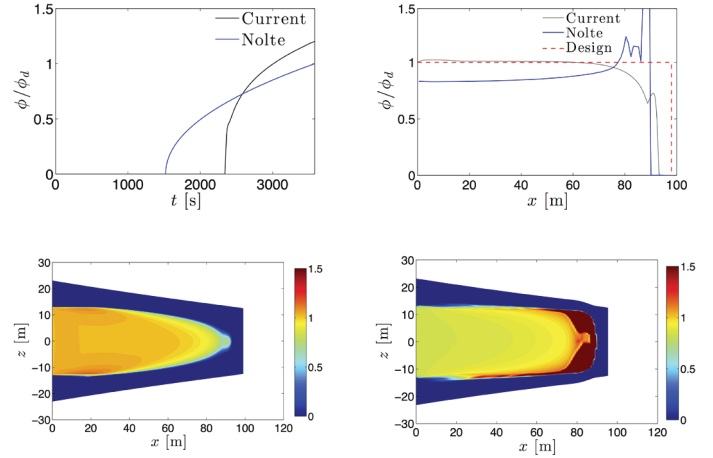


Figure 5. Top left: comparison between the current and Nolte's (efficiency $\eta = 0.39$) pumping schedules for P3D fracture. Top right: comparison between the normalized proppant concentration along the x axis for the current and Nolte's schedules with the design concentration distribution. Bottom left: footprint of the P3D fracture for the current schedule with the color indicating the normalized proppant concentration ϕ/ϕ_d , so that the color associated with 1 corresponds to the desired concentration specified in the design. Bottom right: footprint of the P3D fracture for Nolte's schedule with the color indicating the normalized proppant concentration ϕ/ϕ_d .

on the problem parameters, and in particular on the fracture growth in the vertical direction and the characteristics of the line source implementation in the HF simulator (i.e. the variation of source intensity versus z at $x = 0$). In addition, the developed proppant plug for Nolte's design shown in the bottom right panel in Fig. 5 has a strange shape - the particles are concentrated near the top and the bottom of the fracture, leaving the central part underpropped. Unfortunately, this is due to an inaccuracy in the P3D model as indicated by Adachi et al. (2010), as well as Dontsov and Peirce (2014). The cause of this inaccuracy is that a uniform pressure is assumed along every vertical cross-section, which in turn leads to unrestricted motion of the slurry in the vertical direction. The fact that the slurry is transported to the tip region mainly through the central part of the fracture, and the leakoff occurs uniformly along the height, together lead to strong off-central vertical velocities in the tip region, which move the proppant away from the center to the sides of the fracture. This feature is more pronounced for a smaller particle size, which can reach the region near the fracture tip where most of the leakoff takes place. Larger particles will form a plug some distance away from the crack tip, and are influenced to a much lesser extent; see Dontsov and Peirce (2014). It should be noted that this discussion about particle size can be interpreted as competition between the length scale associated with the leakoff and the distance from the fracture tip to the place at which the fracture width is equal to three particle diameters. The ratio between aforementioned length scales (which depends on many problem parameters) is actually responsible for the separation of "small" and "large" particles in the context of near tip behavior. Note that even though Fig. 5 indicates smaller sensitivity of the proppant placement to the schedule type than Fig. 2, one should always keep in mind that those are the examples for one set of parameters, and some variations are possible for different problem parameters.

To show the capabilities of the proposed scheduling paradigm, Fig 6 shows the pumping schedule and the results of the simulations for regular ($\phi_d = 0.2 \times \phi_m$) and small ($\phi_d = 0.02 \times \phi_m$) concentrations for P3D fractures with "zebra" distributions of proppant. As for the KGD

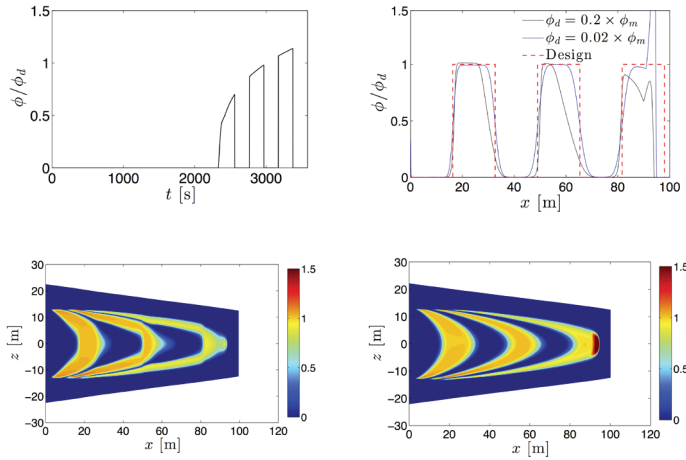


Figure 6. *Top left:* pumping schedule for a so-called “zebra” proppant distribution for the P3D fracture. *Top right:* comparison between normalized proppant concentration along the x axis for regular ($\phi_d = 0.2 \times \phi_m$) and small ($\phi_d = 0.02 \times \phi_m$) concentrations along with the design concentration distribution. *Bottom left:* footprint of the P3D fracture for regular concentration with the color indicating the normalized proppant concentration, ϕ/ϕ_d . *Bottom right:* footprint of the P3D fracture for a small proppant concentration with the color indicating the normalized proppant concentration, ϕ/ϕ_d .

geometry, this “zebra” configuration is defined by requiring a specified proppant placement in three equidistant stripes of the same width along the x axis by the end of the simulation (see Fig. 6). Due to the planar nature of the P3D model, the stripes form an interesting shape, which reflects the velocity pattern inside the fracture. The comparison between the solutions for small and regular concentrations allows estimation of the effect of coupling between proppant transport and HF propagation. This coupling is more pronounced than for the KGD geometry (see Fig. 6) and leads to some notable visual distortions of the proppant pattern, see the bottom panels in Fig. 6. Also, note that both bottom panels in Fig. 6 are not perfectly symmetrical. This is due to the presence of small gravitational settling.

Comments

Comparison between different schedules. While Figs. 2 and 5 show the comparison between Nolte’s schedule and the predictions based on equations (5) and (9), it is instructive to make a comparison for a broader range of efficiencies, η . Fig. 7 compares different schedules: for $\eta = 0.9, 0.5$, and 0.1 .

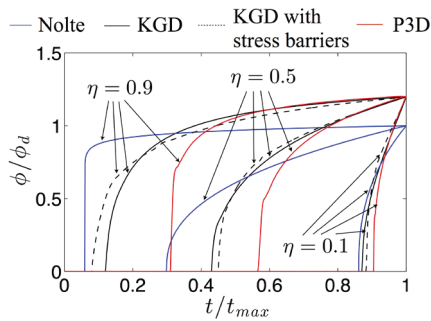


Figure 7. Comparison between different schedules for different values of the efficiency, .

Nolte’s schedules are compared to the corresponding KGD and P3D schedules, as well as to the schedule for a KGD fracture, which is

affected by the presence of symmetric stress barriers. For the purpose of comparison, the stress barriers are placed 60 m from the inlet and have a magnitude $\Delta\sigma = 2.5$ MPa. To achieve the desired value of the efficiency for both KGD and P3D models, the Carter leakoff coefficient is adjusted. The comparison shows significant variability among the different models. As mentioned previously, Nolte’s model underestimates t_p (the time instant at which the proppant is introduced), and the maximum concentration near the end of pumping. What is not clear so far, is the large difference between the schedules for the KGD and P3D geometries. This clearly indicates that there is no universal schedule that can work for all fracture geometries. Even with the same fracture type (KGD), the introduction of stress barriers affects the schedule to some extent. This also supports the fact that a universal schedule can not be generated. One peculiar feature that can be seen from Fig. 7 is the hierarchy between the schedules, namely Nolte’s schedule suggests the earliest proppant injection, followed by the corresponding KGD and, finally, P3D schedules. The difference between Nolte’s and the KGD schedules can be related to the ratio between particle and slurry average velocities, $\beta = 1.2$, which allows the proppant to reach the crack tip faster. At the same time, since the P3D model has another dimension, it effectively introduces another factor, which is the ratio between the peak proppant velocity and the average proppant velocity with respect to the vertical, i.e. the z direction. This can be seen in the bottom panels in Fig. 6. While the proppant at $z = 0$ is already at the tip, on average, the boundary of the corresponding first “zone” of the proppant is some distance away from the tip. The ratio between the peak proppant velocity and average slurry velocity is important, since the former “moves” proppant forward, while the latter is responsible for the fracture growth. This ratio is higher for P3D than for KGD fractures, which allows proppant to reach the crack tip notably faster for a P3D geometry. While the differences between the schedules are prominent for high efficiencies, they become less pronounced for smaller efficiencies, see Fig. 7. Regarding the implementation, Nolte’s schedule is the easiest to deal with since analytical formulas are used. At the same time, once executed, the proposed approach facilitates rapid numerical calculations for either KGD or P3D fractures.

Assumptions and limitations. Despite the fact that the scheduling has been verified numerically, it is essential to understand all of the assumptions behind the model. First, it is assumed that the presence of proppant does not disturb fracture propagation. While this is a critical ingredient for developing a pumping schedule, it limits the applicability to relatively small concentrations, for which the viscosity of the slurry is not significantly perturbed by the presence of proppant particles. However, for the design proppant concentration $\phi_d = 0.2 \times \phi_m$, which was used for the verification, the change in the apparent viscosity is approximately 20%, see the proppant transport model in Dontsov and Peirce (2014). Despite this notable change in the viscosity, Figs. 2 and 5 show good agreement between the target proppant placement and the one that is calculated using the generated schedule. As discussed before, this is due to the fact that the particles spend little time at the near-tip region; since this part of the fracture is primarily responsible for the propagation, the higher slurry viscosity does not substantially alter the fracture footprint. However, due to the nonlinear variation of the slurry viscosity versus particle concentration, higher design concentrations could introduce greater discrepancies. Consequently, it is essential to verify the schedule using numerical simulation. In addition to the reduced accuracy for higher concentrations, the proposed schedule cannot be used for tip screen-out applications, since the proppant plug near the crack tip significantly changes the fracture behavior relative to the corresponding fracture with pure fluid.

The pumping schedule calculation that is proposed in this paper is

always consistent with some hydraulic fracturing model, such as KGD or P3D model. For this reason, it is clear that the correctness of the HF model plays a crucial role in scheduling. This stipulation should not be underestimated, since, according to Fig. 7, there might be a significant difference among various fracture models. In addition, the scheduling is tailored to the specific proppant transport model (see Dontsov and Peirce (2014)), which, in particular, provides the value for β , as is indicated in (1). If one considers a different model, which, for instance, includes the effect of turbulent flow, then the value of β has to be adjusted accordingly.

Possible extensions. One of the biggest advantages of the proposed scheduling procedure is its applicability to multiple hydraulic fracturing models. As an example, a HF simulator with a more accurate leakoff model can be used for the design. Another possibility is to use a HF simulator that accounts for inertial effects near the wellbore. In the latter case, it might be necessary to introduce $\beta(x)$ in (1), since the proppant distribution across the width of the fracture will not resemble its laminar analog, causing the proppant-to-slurry average velocity ratio to change.

Since the accuracy of the proposed scheduling approach deteriorates for higher proppant concentrations, it might be useful to adjust the average velocity history iteratively. In other words, given an initial guess for a schedule, one may run the appropriate HF simulator with proppant and record the history of the average velocity. Then, this velocity history can be used to recalculate a schedule. This process could be repeated until the results converge. Note that the proppant velocity history can be recorded instead of the fluid velocity history, which eliminates the use of β in (1). The current design approach therefore represents the first step in such an iterative process. The iterative approach, although effective, is computationally demanding, and sacrifices the efficacy of the original non-iterative methodology.

Summary

This paper introduces a universal approach for designing a proppant schedule, which complements a given hydraulic fracture simulator. To calculate a schedule, it is assumed that the proppant particles do not affect the fracture propagation until they reach the tip region and cause proppant plug formation. This makes it possible to “pre-compute” the history of the velocity distribution assuming *no proppant*. This is then used to evaluate the prospective proppant movement. Once the prospective movement is calculated, volume balance is used to relate the desired proppant concentration at a given point in space (the concentration does not have to be uniform) to a corresponding input concentration at a certain time instant. In this way, the schedule is obtained without solving an inverse problem. The scheme is illustrated for two fracture geometries; namely, KGD and P3D. It is shown that Nolte’s schedule suggests earlier proppant injection, which leads to a premature tip screen-out, while the current approach produces more accurate results and does not alter the desired final fracture half-length. In addition, the effect of coupling between proppant transport and hydraulic fracture propagation is studied. As expected, smaller proppant concentrations lead to more accurate results, while the agreement for higher concentrations is still adequate. The comparison between the schedules for different fracture geometries together with Nolte’s schedule for different efficiencies shows that knowledge of the efficiency alone is not sufficient to predict the schedule. In particular, a noticeable difference is observed between all of the models considered. This demonstrates that although there is no universal schedule that is applicable to multiple fracture geometries, the proposed technique is able to accurately and rapidly generate an optimal pumping schedule.

Acknowledgments

The support of the British Columbia Oil and Gas Commission and the NSERC discovery grants program is gratefully acknowledged.

Appendix: Nolte’s pumping schedule

This appendix summarizes Nolte’s pumping schedule that is used in this paper for comparison purposes. As follows from Nolte (1986), the proppant concentration, which should lead to uniform distribution of proppant at the end of the fracturing job, can be written as

$$\phi(t) = \phi_d \left(\frac{t - t_p}{t_e - t_p} \right)^{1 - \eta - f_d/\eta}, \quad t > t_p,$$

where ϕ_d is the design concentration, t_e is the total injection time of the fluid and slurry, $t_p = ((1 - \eta)^2 + f_d)t_e$ is the time at which proppant is introduced, η denotes the efficiency calculated as the ratio between the volume of the fracture and the total volume that is injected, and $f_d = 0.05$ is a correction factor. As discussed in Nolte (1986), this correction factor makes it possible to match the data obtained through numerical simulations. Note that it is implicitly assumed that $\phi(t) = 0$ for $t < t_p$.

Nomenclature

l_e	= fracture design half-length
t_e	= total injection time
t_p	= “pad” time
w	= fracture width
V_f	= average fluid velocity for KGD fracture
$x(t, t_i)$	= position of the particles at time t , injected at time t_i
$\beta = 1.2$	= the ratio between proppant and fluid average velocities for small particle concentration
ϕ	= proppant volume fraction
Q_0	= slurry injection rate
a	= particle radius
$\phi_{d(x)}$	= design proppant concentration distribution inside the fracture
$\phi_d = 0.585$	= maximum volume fraction of proppant
η	= efficiency
$V_{f,x}, V_{f,z}$	= lateral and vertical average fluid velocity components for P3D fracture

References

- J. Adachi, E. Siebrits, A. Peirce, and J. Desroches. Computer simulation of hydraulic fractures. *Int. J. Rock Mech. Min. Sci.*, 44:739–757, 2007.
- J. I. Adachi, E. Detournay, and A. P. Peirce. An analysis of classical pseudo-3D model for hydraulic fracture with equilibrium height growth across stress barriers. *Int. J. of Rock Mech. and Min. Sci.*, 47:625–639, 2010.
- F. Boyer, E. Guazzelli, and O. Pouliquen. Unifying suspension and granular rheology. *Phys. Rev. Lett.*, 107: 188301, 2011.
- C.L. Cipolla, E. P. Lolon, M.J. Mayerhofer, and N.R. Warpinski. The effect of proppant distribution and un-propped fracture conductivity on well performance in unconventional gas reservoirs. In *SPE Hydraulic Fracturing Technology Conference*, 2009.
- H.R. Crawford. Proppant scheduling and calculation of fluid lost during fracturing. In *SPE Annual Technical Conference and Exhibition*, 1983.

- A.A. Daneshy. Numerical solution of sand transport in hydraulic fracturing. *J. Pet. Tech.*, pages 132–140, 1978.
- E.V. Dontsov and A.P. Peirce. Proppant transport in hydraulic fracturing: Crack tip screen-out in KGD and P3D models. <http://hdl.handle.net/2429/46109>, 2014.
- M.J. Economides and K.G. Nolte, editors. *Reservoir Stimulation*. John Wiley & Sons, Chichester, UK, 3rd edition, 2000.
- H. Gu and J. Desroches. New pump schedule generator for hydraulic fracturing treatment design. In *SPE Latin American and Caribbean Petroleum Engineering Conference*, 2003.
- H.Z. Meng and K.E. Brown. Coupling of production forecasting, fracture geometry requirements and treatment scheduling in the optimum hydraulic fracture design. In *SPE Low Permeability Reservoirs Symposium*, 1987.
- A.T. Mobbs and P.S. Hammond. Computer simulations of proppant transport in a hydraulic fracture. *SPE Prod. Facil.*, pages 112–121, 2001.
- L.B. Neto and A. Kotousov. On the residual opening of hydraulic fractures. *Int. J. Fract.*, 181:127–137, 2013.
- K.G. Nolte. Determination of proppant and fluid schedules from fracturing-pressure decline. *SPE Prod. Eng.*, pages 255–265, 1986.
- A. Peirce and E. Detournay. An implicit level set method for modeling hydraulically driven fractures. *Comput. Methods Appl. Mech. Engrg.*, 197:2858–2885, 2008.
- M. M. Rahman and M. K. Rahman. A review of hydraulic fracture models and development of an improved pseudo-3D model for stimulating tight oil/gas sand. *Energy Sources, Part A*, 32:1416–1436, 2010.
- E.M. Shokir and A.A. Al-Quraishi. Experimental and numerical investigation of proppant placement in hydraulic fractures. In *SPE Latin American and Caribbean Petroleum Engineering Conference*, 2007.

Biographies



Egor Dontsov is a Postdoctoral Fellow in the Department of Mathematics at the University of British Columbia, Canada. He received his bachelor degree in Physics from Novosibirsk State University in Russia in 2008. Then, Egor moved to Minneapolis, USA, where he received PhD in Civil Engineering at the University of Minnesota in 2012. His thesis was devoted to nonlinear ultrasound wave propagation with applications to medical imaging. His current research interests are in the area of hydraulic fracturing. In particular, he focuses on the numerical modeling of hydraulic fracture propagation, as well as investigation of proppant transport inside them.



Anthony Peirce is a Professor in the Department of Mathematics at the University of British Columbia, Canada. He was a Fulbright Scholar at Princeton University, where he received his PhD in Applied and Computational Mathematics in 1987. Prior to his PhD, he worked as an Applied Mathematician at the Chamber of Mines Research Laboratories in South Africa, where he investigated rock fracture processes around underground excavations. His research interests include: the application of control to molecular systems, the analysis of instabilities in elasto-plastic materials, the development of specialized numerical algorithms to model large-scale rock fracture processes, numerical and analytic studies of reactive flows in porous media, and more recently, the asymptotic and numerical analysis of fluid-driven-fracture propagation. Further details are available on his website: www.math.ubc.ca/~peirce